Influence of endotoxin-mediated retinal inflammation on phenotype of diabetic retinopathy in *Ins2*^{Akita} mice

Nermina N. Vagaja (PhD)[1,2] , Nicolette Binz (PhD)[2], Samuel McLenachan (PhD)[3], Elizabeth P. Rakoczy (PhD)[1,2] , Paul G. McMenamin (DSc(Med))[4]

[1]Centre for Ophthalmology and Visual Science, The University of Western Australia, Crawley WA 6009, Australia

[2] Department of Molecular Ophthalmology, Lions Eye Institute, Nedlands, WA 6009, Australia

[3]Ocular Tissue Engineering Laboratory, Lions Eye Institute , Nedlands, WA 6009, Australia

[4]Department of Anatomy and Developmental Biology, School of Biomedical Sciences, Monash University, Clayton, VIC 3800

Correspondence to:

Professor Paul G McMenamin D.Sc.(Med)

Department of Anatomy & Developmental Biology

School of Biomedical Sciences, Faculty of Medicine, Nursing and Health Sciences

Monash University, Building 13C, Wellington Rd, Clayton, Victoria, 3800, Australia

paul.mcmenamin@monash.edu Ph +613 99056219

Short title: Systemic endotoxaemia induces changes in the diabetic retina

Funding: NHMRC Australia Grant No **634469**

Conflicting Interests: The authors declare there are no conflicting or competing interests pertaining to this manuscript.

Figures: 5

Word count (main text): 2841

ABSTRACT

Aims: The purpose of this study is to evaluate the impact of systemic exposure to bacterial lipopolysaccharide (LPS) on the C57BL6/J-*Ins2*^{Akita} mouse, a rodent model of background diabetic retinopathy.

Methods: Toll-like receptor 4 (TLR4) mediated systemic inflammation was induced in *Ins2*^{Akita} heterozygotes and age-matched C57BL6/J-*Ins2*$^{+}$ littermates by single or repeated intraperitoneal injections of the TLR4 ligand lipopolysaccharide (LPS, 9µg/g body weight). Twenty four hours after a single injection in 7 week old mice retinal *Il1b*, *Tnfa* and *Vegf* transcripts were measured with real-time PCR. VEGF protein levels were evaluated with bead-based immunoassay. Leukostasis and endothelial injury were assessed in retinal wholemounts following perfusion with rhodamine- or FITC-conjugated concanavalin A to label leukocytes and propidium iodide to label dead or injured cells. In mice which had received three fortnightly injections between 10 and 16 weeks of age, retinal thicknesses and vascular structure were evaluated at 17-18 weeks of age using optical coherence tomography (OCT) and fluorescein angiography. Retinal architecture and cell densities were assesed using resin-based histology.

Results: Compared with normoglycaemic C57BL6/J-*Ins2*$^{+}$ controls, systemic LPS exposure in *Ins2*^{Akita} mice was associated with a 3.5-fold increase in endothelial cell injury and attenuated (54%) reactive leukostasis in the retinal vasculature. Hyperglycaemia or acute LPS-inflammation did not increase retinal VEGF content. Thinning (10-13µm) of posterior retina was detected with OCT two weeks after repeated exposure to LPS in *Ins2*^{Akita} mice but not in normoglycaemic controls. Capillary networks and retinal morphology were unaffected by recurrent LPS-inflammation in *Ins2*^{Akita} and control mice.

Conclusion: In hyperglycaemic mice, exposure to systemic LPS was associated with two hallmark pathologies of early background DR, namely, the injury of capillary endothelium and when repeated three times, with *in vivo* thinning of the retina.

INTRODUCTION

Chronic sterile tissue inflammation [1] is the fundamental process that underlies dysfunction, injury and remodeling of tissues affected by common degenerative conditions like atherosclerosis, coronary artery disease and cerebrovascular disease.[1, 2] In diabetes, glucotoxic injury of the retina is associated with chronic retinal inflammation, which manifests as leukostasis, activation of microglia, vascular hyperpermeability and increased production of inflammatory mediators.[3] Several lines of evidence suggest that in the context of hyperglycemia, inflammatory responses may contribute to the degeneration of retinal capillaries which represents the first stage of microvascular remodeling in diabetic retinopathy (DR).[3] However, a critical amount of retinal capillary dropout, which would potentially result in tissue hypoxia and spontaneous preretinal neovascularization, has not yet been achieved in commonly used rodent models of DR.[3]

Common causes of systemic inflammation, such as bacterial infection, have been linked in several instances to worsening of tissue dysfunction or injury in central nervous system (CNS) and cardiovascular degeneration. Specifically, systemic infections exacerbate neurodegenerative conditions such as Alzheimer's disease, and Parkinson's disease [4] and can increase the risk of stroke and coronary artery disease.[5]

In diabetic patients, elevated circulating inflammatory markers correlate with microvascular complications,[6] including DR.[7-9] Furthermore, a small number of studies have suggested an association between distant infections and acceleration of DR. An increased risk of retinopathy has been reported in diabetic subjects with periodontal disease [10] and bacteriuria.[11] Rapid progression of DR has been reported in humans during West Nile virus infection [12] and after recovery from sepsis-related endophthalmitis [13, 14] but the mechanisms for this are unclear. Given the increasingly recognized importance of retinal inflammation in the pathophysiology of DR, together with the concept that infections exacerbate chronic illnesses in other organ systems, we saw the need to evaluate the potential of systemic sources of inflammation to accelerate the pathogenesis of DR. Accordingly, the aim of the present study was

to evaluate the effects of systemic exposure to bacterial lipopolysaccharide (LPS) on inflammatory markers, vasculature and morphological integrity of the retina in 7-18 week old *Ins2*^{Akita} mouse model of background DR.

MATERIALS AND METHODS

Experimental mice. Male C57BL6/J-*Ins2*^{Akita} heterozygotes [15, 16] and age-matched C57BL6/J-*Ins2*$^{+}$ male littermates, herein referred to as *Ins2*^{Akita} and wild type (WT) mice respectively, were derived from commercially available breeders (Jackson Laboratories, Bar Harbor, ME). The mice were housed and genotyped for the *Ins2*^{Akita} and *rd8* mutation in the *Crb1* gene as previously described.[17, 18] The experimental diabetic animals were not treated with insulin. Mice were sacrificed either at 7 or at 18 weeks of age with a lethal dose of intraperitoneal (i.p.) sodium pentobarbitone (150 mg/kg body weight).

Glycaemic status

Non-fasting blood glucose level (BGL) and glycosylated haemoglobin (HbA1c) were measured at death, using previously described methods.[19]

LPS injections.

Ultra-pure *E.coli* LPS (Strain K12, Invivogen, San Diego, CA, USA.) was diluted to 10µg/µL in pyrogen-free phosphate buffered saline (PBS) for injections (Pfizer, Bentley, WA, Australia) and injected at 9µg/g body weight. To study the short-term effects of acute inflammation, 6-7 week old *Ins2*^{Akita} and their normoglycaemic WT littermates were injected intraperitoneally (i.p.) with LPS or PBS and sacrificed 24 hours later. To model recurrent systemic inflammation secondary to repeated bacterial infections, a separate group of *Ins2*^{Akita} and WT mice received three fortnightly doses of LPS or PBS, starting from 10-11 weeks of life. A 2 week interval was allowed between the final injection and death at 17-18 weeks of age.

Evaluation of *ex-vivo* leukostasis.

After transcardial perfusion with 20ml PBS the whole body was fixed with 10 ml 2% paraformaldehyde (PFA), followed by 5ml of Rhodamine-conjugated Concanavalin A or FITC Concanavalin A (12.5µg/ml in PBS; Vector, Burlingame, CA, USA) and 10 ml PBS (N=7-12 mice/group). Eyes were post-fixed in 2% PFA for two hours at room temperature (RT). Whole retinae, mounted in PBS vitreous side up, were

examined by epifluorescence microscopy (Olympus BX60, Tokyo, Japan) with 40x objective and the total number of adherent leukocytes per retina was determined. Epifluorescence microscopy was also employed to examine the Concanavalin-A stained microvasculature for evidence of microaneurysms or capillary dropout

Ex vivo analysis of endothelial injury

Acutely endotoxic mice and PBS controls were injected i.p. with 400µg of P.I. (Sigma-Aldrich, Castle Hill, NSW, Australia) in pyrogen-free saline, one hour preceding death and transcardial perfusion with FITC-Concanavalin A as described above. The P.I. positive cells were quantified from whole retinal flatmounts using epifluorescence microscopy (n=7-10 mice/group) and x40 magnification, under 470-490nm excitation filter.

RT reaction and real-time quantitative PCR

Right and left retinae from individual mice were pooled into one sample per mouse. Total RNA was extracted using the RNeasy Mini Kit (Qiagen) and treated with DNAse I (Qiagen) according to manufacturer's instructions. The RNA was reverse-transcribed using the high capacity RNA-to-cDNA Kits (Applied Biosystems, Mulgrave VIC, Australia). Real-time PCR reactions were performed in triplicate, on the Rotorgene 3000 thermal cycler, with predesigned TaqMan® Gene Expression Assays (Applied Biosystems) according to manufacturer's instructions. Peptidylprolyl isomerase A (Ppia) was used as endogenous housekeeping gene.

Protein quantitation. Bead-based immunoassay technology (xMAP TM, Luminex, Austin TX, USA) was used to determine concentrations of murine VEGF from retinal protein extracts. The pre-made Procarta Mouse Cytokine Profiling Kit was used according to manufacturer's instructions. Each sample was tested in duplicate with 125µg of total protein per replicate.

Conventional histology. Digital images of 5µm thick Haematoxylin and Eosin (H&E) stained glycomethacrylate resin sections of mouse eyes in the pupillary-optic nerve axis were used to measure (by a masked observer) cell nuclei in the INL and ONL using the ruler tool in ImageScope software

(version11.0.2.725, Aperio Technologies, Vista, CA, USA). Cell nuclei were counted in 20µm wide columns centered over reference lines perpendicular to the retina, which were at 300, 600 and 900µm from the optic axis and the peripheral margins of the retina. The nuclei in the GCL were counted along the 300µm distance between reference lines.

Clinical ophthalmic photography. Confocal laser scanning ophthalmoscopy (cSLO) and OCT were performed on 17-18 week old mice using a Spectralis HRAII with OCT (Heidelberg Engineering, Dossenheim, Germany), as described before[19] with some modifications. Fluorescein angiograms of deep and intermediate capillary networks were exported as TIF files (1536 x 1636 pixels, resolution 0.6635µm/pixel). Using Adobe Photoshop (Version 7.0, Adobe Systems, San Jose, SA, USA), three sample regions (240 x 240 pixels) containing capillaries within 800µm radius from the optic cup were randomly extracted from TIFs. Vascular outlines were manually traced in sample regions using Adobe Photoshop. Binary images of sample regions were generated and skeletonised using ImageJ software (v.1.44p, National Institutes of Health, Bethesda, MD, USA), followed by a standard box-count analysis using the FracLac plugin (v2.5 Release 1e). Fractal dimensions were averaged for each mouse before statistical analysis. Retinal thickness was measured at 300, 600 and 900µm from the optic cup employing B-scans of the nasal and temporal quadrant.All image manipulations were performed in a masked manner.

Statistical analysis. One-way ANOVA, followed by Bonferroni's Multiple Comparison Test at a 5% significance level was performed using GraphPad Prism Version 4.01 for Windows (GraphPad Software, San Diego, CA, USA). Data are presented as mean ± standard error of mean (SEM), except for blood glucose levels and glycosylated haemoglobin which are expressed as mean ± standard deviation (SD).

RESULTS

Effect of LPS on glycaemic status of *Ins2*^{Akita} mice

Non-fasting BGL (mmol/L) and HbA1c% were significantly higher in 7 week old *Ins2*^{Akita} -PBS injected mice than in WT-PBS injected littermates, consistent with the onset of hyperglycaemia (Figure 1 A and B, respectively). Short-term (24 hour) exposure to i.p. LPS did not alter the BGL, nor the HbA1c%, in non-diabetic WT-LPS mice from control WT-PBS mice, however BGL in diabetic *Ins2*^{Akita}-LPS mice dropped significantly in comparison to PBS-control *Ins2*^{Akita} mice (Figure 1A and B respectively).

HbA1c% was unchanged between 18 week old WT-PBS and WT-LPS mice. Although pathologically elevated, mean HbA1c% in 18 week old *Ins2*^{Akita} mice which received three injections of LPS was significantly lower than HbA1c% in PBS-treated *Ins2*^{Akita} mice (Figure 1C).

Measurement of acute LPS-induced endothelial injury in early background DR

The use of P.I. fluorescence revealed injured or dead retinal endothelial cells, which typically presented as a single P.I.$^{+}$ capillary loop or a cluster of P.I.$^{+}$ capillary loops in the mid-periphery of the retinae of LPS-treated mice (Figure 2A,C,D). P.I. labeling of endothelial cells was very low in both diabetic mice and non-diabetic controls injected with PBS. However, 24 hours after LPS, the number of P.I.$^{+}$ cells increased in the retinal vasculature of both WT and *Ins2*^{Akita} mice. The LPS-induced endothelial cell injury was significantly greater in *Ins2*^{Akita}-LPS mice from that in WT-LPS mice ($p<0.05$)(Figure 2B) showing that hyperglycaemia exacerbates this effect.

Measurement of acute LPS-induced leukostasis in retinae of *Ins2*^{Akita} mice

The numbers of adherent retinal leukocytes per retina were similar in 7 week old PBS-treated WT and *Ins2*^{Akita} mice (Figure 3 A, B, D, F). Twenty-four hours after LPS injection significant retinal leukostasis developed in both normoglycaemic WT and *Ins2*^{Akita} mice, in comparison to PBS-treated controls (Figure

3C,E,F). However, reactive leukostasis was significantly attenuated in LPS-treated *Ins2*^{Akita} mice, when compared to controls (Figure 3F). These results demonstrate that reactive retinal leukostasis develops in mice 24 hours after the i.p. injection of LPS, and that this response is subdued in diabetic mice which had been hyperglycaemic for around 3-4 weeks.

Characterisation of the acute inflammatory response to i.p. LPS in retinae of *Ins2*^{Akita} mice

There was no significant difference in neuroretinal expression of markers of inflammation *Il1b* mRNA or *Tnfa* mRNA between WT-PBS and *Ins2*^{Akita}-PBS mice. Compared to PBS-controls, LPS administration was associated with a significant induction of retinal *Il1b* and *Tnfa* transcripts in both normoglycaemic and diabetic mice, which did not significantly differ between *Ins2*^{Akita}-LPS and WT-LPS mice. *Icam1* was similarly upregulated in WT-LPS mice and in *Ins2*^{Akita}-LPS mice in comparison to PBS controls. Systemic LPS, diabetes or a combination of both did not significantly change the expression of retinal *Cd18* (See Supplementary Figure 1, available online only).

Retinal Vegf response to hyperglycaemia and i.p. LPS

A 2-3 week history of hyperglycaemia in 7 week old PBS-treated *Ins2*^{Akita} mice was associated with 34% reduction of neuroretinal *Vegf* mRNA and 17% reduction of neuroretinal VEGF protein when compared to PBS-WT controls. Administration of LPS to WT mice was also associated with significant reduction (27%) of retinal *Vegf* mRNA and 18% decrease in the abundance of retinal VEGF protein (vs PBS-WT)(See Supplementary Figure 2, available online only). Together, these results demonstrate that a reduction in retinal VEGF expression can result from either short-term hyperglycemia or acute exposure to LPS.

Effect of recurrent exposure to LPS on retinal thickness in early background DR

In vivo analysis of retinal thickness with OCT (Figure 4A-C) revealed a significant but minor thinning of central retina in 18 week old *Ins2*^{Akita} mice after three doses of LPS spread over six weeks, two weeks after last injection, specifically at 300µm and 600µm distances from the optic cup, when compared to matching locations in LPS-treated normoglycaemic WT mice (Figure 4D and 6E, respectively). Neither recurrent

exposure to LPS in WT mice, nor 14 weeks of diabetes in PBS-treated *Ins2*^{Akita} mice significantly affected the total thickness of the central retina (Figure 4D-F). Detailed nuclear counts, which were performed using high quality resin-embedded sections, did not reveal significant differences between the experimental groups (data not shown) reducing the likelihood of outer nuclear layers as sources of the thinning of total retina.

Recurrent LPS and capillary regression in early background DR

Retinal fluorescein angiograms and fractal analysis of the deep and intermediate capillary networks revealed no significant difference in in vessels between the four experimental groups (Figure 5E-F). There was no evidence of retinal leakage of fluorescein between these groups. No morphological differences were found on qualitative-post mortem assessment of Concanavalin A stained retinal microvasculature.

DISCUSSION

In light of the increasingly accepted concept that tissue inflammation plays a significant role in the pathogenesis of DR[3] we sought to test the hypothesis that systemic exposure to gram negative ultra-pure TLR4 specific endotoxin (LPS) would activate the innate inflammatory injury of the retina of diabetic *Ins2*^{Akita} mice. Our data revealed that an acute (24 hours) response to systemic LPS caused greater retinal endothelial injury in diabetic *Ins2*^{Akita} mice than in identically treated WT littermates, which was associated with reactive LPS-leukostasis being suppressed in diabetic mice. Our data revealed a small but measurable thinning of the central retina in *Ins2*^{Akita} mice following repeated exposure to LPS.

Our findings of acute injury to the retinal endothelium in LPS-treated WT (C57BL6/J-*Ins2*$^{+}$) and *Ins2*^{Akita} mice support previous observations of LPS-induced endothelial injury in rat retina [20] and suggest that activation of TLR4-dependent innate immune responses causes focal retinal capillary damage in both the non-diabetic and diabetic retina. Importantly, in our study we noted a heightened susceptibility to acute LPS-induced injury of the endothelium in *Ins2*^{Akita} mice even after a short (2-3 week) history of diabetes, supporting the hypothesis that gram negative infections can encourage microvascular injury in adults with minimal DR. Our study did not evaluate whether LPS-induced changes in blood pressure contributed to this injury. Furthermore, clinically relevant vasoregression was not observed in *Ins2*^{Akita} mice even after repeated doses of LPS. Possible reasons for lack of vasoregression after repeated LPS were insufficient severity and duration of LPS effects, the selective (TLR4) activation of inflammatory response, and the relatively short duration of pre-existing diabetes in this mouse model. Similar experiments in older *Ins2*^{Akita} mice would be required to examine the possible development of symptoms of advanced DR in these mice.

With the increasing availability of OCT technology, multiple studies have demonstrated retinal thinning (9-14µm) primarily of the inner layers of the central and pericentral macula, as one of the earliest clinical signs of human DR, which precedes detectable retinal capillary dropout.[21] Although others have reported histological thinning and gross disruption of neural architecture in the retinae of 26 week old *Ins2*^{Akita}

mice,[16] we could not replicate these findings using either clinical OCT imaging or histological analysis. In parallel studies, retinal thinning or degeneration was not observed in *Ins2*^{Akita} mice up to 25 weeks of age,[22] demonstrating that hyperglycemia alone is insufficient to induce retinal thinning in this mouse model. However, with the aid of OCT, we were able to detect significant thinning of posterior retina (10-13µm or 3-5%) in 18 week old *Ins2*^{Akita} mice after three doses of LPS. This finding raises the possibility that TLR4-mediated innate immune activation contributes to premature retinal thinning in diabetes. Although we cannot rule out retinal thinning in *Ins2*^{Akita} mice past 26 weeks of age, our results suggest that additional factors, such as the presence of infections may possibly be unrecognized factors necessary to induce or accelerate the appearance of advanced, clinically-detectable retinal pathology in *Ins2*^{Akita} mouse colonies.

Our study shows that adherent retinal leukocytes in the retina are similar in 7 week old PBS-treated WT and Ins2^{Akita} mice, with the latter group being hyperglycaemic for four weeks. These findings diverge from prior reports of significant retinal leukostasis developing within few days to weeks from the onset of hyperglycaemia in streptozotocin-induced rodent models of diabetes.[23, 24] However, the currently available literature does not clarify if streptozotocin contributes to retinal leukostasis *per se* or via the systemic toxicity including hepatotoxicity [25, 26] and nephrotoxicity.[27] It is also unclear if streptozotocin-insulitis involves a significant enough acute phase response that could trigger retinal leukostasis. By using a mouse model of spontaneous onset diabetes, like the Ins2^{Akita} mouse, these possible confounding effects of toxin-induced diabetes are excluded, which we believe is a strength of the present study.

The LPS-induced leukostasis we observed in *Ins2*^{Akita} mice was attenuated in comparison to LPS-treated WT mice, confirming previous findings of impaired leukostasis in streptozotocin-diabetic rats after systemic LPS.[28] Similar diminished response by leukocytes was observed in diabetic rat retina 24 hours after ischaemia reperfusion injury.[29] Our findings reinforce the notion that responses of leukocytes to inflammation or injury in diabetic retina are blunted, [28] however the relevant underlying mechanisms for this are unclear. Importantly, a range of abnormal leukocyte behaviours has been reported in non-ocular

diabetic tissues, for instance decreased chemotactic responses of neutrophils to inflammatory mediators, impaired adhesion to the endothelium and increased apoptosis,[30] all changes that may underlie the attenuation of leukostasis after LPS-induced inflammation observed here and reperfusion injury reported previously in diabetic retina. [29]

To our knowledge, this is the first study that has measured retinal *Vegf* transcript and protein after a relatively short history of diabetes in a mouse model with spontaneous onset of hyperglycaemia. Given the anti-apoptotic properties of VEGF, reduced expression of this factor could be involved in previously reported caspase activation in retinae of 8 week old *Ins2*^{Akita} mice.[16] Furthermore, our finding that expression of retinal VEGF is reduced acutely after LPS exposure in a healthy mouse corresponds to a previously reported decline in tissue expression of VEGF in the mouse brain, lung, kidney and spleen, 24 hours after systemic LPS.[31]

In summary, the central hypothesis in this study was that diabetes would predispose the retina to acute and chronic injury from a mimic of systemic infection and that such injuries might accelerate the onset and progression of diabetic retinopathy. Our data reveals that LPS-induced systemic inflammation result in damage to retinal vessels and, if repeated, contributes to retinal thinning in mice with diabetic *Ins2*^{Akita} mice. We confirm previous findings of abnormal reactive leukostasis in response to LPS in diabetic retina, indicating an altered inflammatory response. Subsequent studies will be required to evaluate if other triggers of innate inflammation (especially other TLR ligands) in the retina can more efficiently accelerate the background DR in mice, with the aim of producing a more advanced retinal pathology than what is found in current slowly progressing models. These studies are in progress. Further studies may also clarify if longer durations of hyperglycaemia and established tissue pathology predispose the retina to a more significant pathogen-mediated injury.

REFERENCES

1.Chen GY, Nunez G. Sterile inflammation: sensing and reacting to damage. Nat Rev Immunol. 2010;**10**(12):826-37.

2.Mann DL. The emerging role of innate immunity in the heart and vascular system: for whom the cell tolls. Circ Res. 2011;**108**(9):1133-45.

3.Tang J, Kern TS. Inflammation in diabetic retinopathy. Prog Retin Eye Res. 2011;**30**(5):343-58.

4.Perry VH, Cunningham C, Holmes C. Systemic infections and inflammation affect chronic neurodegeneration. Nat Rev Immunol. 2007;**7**(2):161-7.

5.Smeeth L, Thomas SL, Hall AJ, et al. Risk of myocardial infarction and stroke after acute infection or vaccination. N Engl J Med. 2004;**351**(25):2611-8.

6.Devaraj S, Cheung AT, Jialal I, et al. Evidence of increased inflammation and microcirculatory abnormalities in patients with type 1 diabetes and their role in microvascular complications. Diabetes. 2007;**56**(11):2790-6.

7.Zorena K, Mysliwska J, Mysliwiec M, et al. Serum TNF-alpha level predicts nonproliferative diabetic retinopathy in children. Mediators Inflamm. 2007;**2007**:92196.

8.Gustavsson C, Agardh E, Bengtsson B, et al. TNF-alpha is an independent serum marker for proliferative retinopathy in type 1 diabetic patients. J Diabetes Complications. 2008;**22**(5):309-16.

9.Klein BE, Knudtson MD, Tsai MY, et al. The relation of markers of inflammation and endothelial dysfunction to the prevalence and progression of diabetic retinopathy: Wisconsin epidemiologic study of diabetic retinopathy. Arch Ophthalmol. 2009;**127**(9):1175-82.

10.Noma H, Sakamoto I, Mochizuki H, et al. Relationship between periodontal disease and diabetic retinopathy. Diabetes Care. 2004;**27**(2):615.

11.Vejlsgaard R. Studies on urinary infection in diabetics. II. Significant bacteriuria in relation to long-term diabetic manifestations. Acta Med Scand. 1966;**179**(2):183-8.

12.Khairallah M, Ben Yahia S, Attia S, et al. Severe ischemic maculopathy in a patient with West Nile virus infection. Ophthalmic Surg Lasers Imaging. 2006;**37**(3):240-2.

13.Lai TY, Kwok AK, Lam DS, et al. Progression of diabetic retinopathy after endophthalmitis. Ophthalmology. 2000;**107**(4):619-21.

14.Tan CS, Yap EY. Rapid progression of diabetic retinopathy following endophthalmitis. Eye (Lond). 2004;**18**(10):1013-5.

15.Wang J, Takeuchi T, Tanaka S, et al. A mutation in the insulin 2 gene induces diabetes with severe pancreatic beta-cell dysfunction in the Mody mouse. J Clin Invest. 1999;**103**(1):27-37.

16.Barber AJ, Antonetti DA, Kern TS, et al. The Ins2Akita mouse as a model of early retinal complications in diabetes. Invest Ophthalmol Vis Sci. 2005;**46**(6):2210-18.

17.Vagaja NN, Chinnery HR, Binz N, et al. Changes in murine hyalocytes are valuable early indicators of ocular disease. Invest Ophthalmol Vis Sci. 2012;**53**(3):1445-51.

18.Mattapallil MJ, Wawrousek EF, Chan CC, et al. The Rd8 Mutation of the Crb1 Gene Is Present in Vendor Lines of C57BL/6N Mice and Embryonic Stem Cells, and Confounds Ocular Induced Mutant Phenotypes. Invest Ophthalmol Vis Sci. 2012;**53**(6):2921-7.

19.Rakoczy EP, Ali Rahman IS, Binz N, et al. Characterization of a mouse model of hyperglycemia and retinal neovascularization. Am J Pathol. 2010;**177**(5):2659-70.

20.Koizumi K, Poulaki V, Doehmen S, et al. Contribution of TNF-alpha to leukocyte adhesion, vascular leakage, and apoptotic cell death in endotoxin-induced uveitis in vivo. Invest Ophthalmol Vis Sci. 2003;**44**(5):2184-91.

21.Van Dijk HW, Verbraak FD, Kok PH, et al. Decreased Retinal Ganglion Cell Layer Thickness in Type 1 Diabetic Patients. Invest Ophthalmol Vis Sci. 2010;**51**(7):3660-5.

22.McLenachan S, Chen X, McMenamin P, et al. Hyperglycemia Induced Glial Reactivity in the Ins2Akita Retina Occurs in the Absence of Clinical Correlates of Diabetic Retinopathy. Clin Exp Ophthalmol 2013;**CEO-12-08-0679**.

23.Miyamoto K, Khosrof S, Bursell SE, et al. Prevention of leukostasis and vascular leakage in streptozotocin-induced diabetic retinopathy via intercellular adhesion molecule-1 inhibition. Proc Natl Acad Sci U S A. 1999;**96**(19):10836-41.

24.Serra AM, Waddell J, Manivannan A, et al. CD11b+ bone marrow-derived monocytes are the major leukocyte subset responsible for retinal capillary leukostasis in experimental diabetes in mouse and express high levels of CCR5 in the circulation. Am J Pathol. 2012;**181**(2):719-27. Epub 2012/06/09.

25.Kume E, Aruga C, Ishizuka Y, et al. Gene expression profiling in streptozotocin treated mouse liver using DNA microarray. Experimental and toxicologic pathology : official journal of the Gesellschaft fur Toxikologische Pathologie. 2005;**56**(4-5):235-44. Epub 2005/04/09.

26.Kume E, Fujimura H, Matsuki N, et al. Hepatic changes in the acute phase of streptozotocin (SZ)-induced diabetes in mice. Experimental and toxicologic pathology : official journal of the Gesellschaft fur Toxikologische Pathologie. 2004;**55**(6):467-80. Epub 2004/09/24.

27.Hall-Craggs M, Brenner DE, Vigorito RD, et al. Acute renal failure and renal tubular squamous metaplasia following treatment with streptozotocin. Hum Pathol. 1982;**13**(6):597-601. Epub 1982/06/01.

28.Tamura H, Kiryu J, Miyamoto K, et al. In vivo evaluation of ocular inflammatory responses in experimental diabetes. Br J Ophthalmol. 2005;**89**(8):1052-7.

29.Tsujikawa A, Kiryu J, Nonaka A, et al. Leukocyte-endothelial cell interactions in diabetic retina after transient retinal ischemia. Am J Physiol Regul Integr Comp Physiol. 2000;**279**(3):R980-9.

30.Alba-Loureiro TC, Munhoz CD, Martins JO, et al. Neutrophil function and metabolism in individuals with diabetes mellitus. Braz J Med Biol Res. 2007;**40**(8):1037-44.

31.Yano K, Liaw PC, Mullington JM, et al. Vascular endothelial growth factor is an important determinant of sepsis morbidity and mortality. J Exp Med. 2006;**203**(6):1447-58.

FIGURE LEGENDS

Figure 1. Glycaemic status at time of death. (A) Random blood glucose and (B) glycosylated haemoglobin in 7 week old mice, 24 hours after a single injection of PBS or LPS. **(C)** Glycosylated haemoglobin in 18 week old mice which received three fortnightly injections of PBS or LPS. Data are presented as mean ± SD. N=7-13 mice per group. Abbreviations: WT – wild type C57BL6/J-*Ins2*$^{+}$, AK – *Ins2*^{Akita}, LPS – lipopolysaccharide, PBS – phosphate-buffered saline.

Figure 2. Epifluorescent microscopy of FITC-Con A perfused retinal whole mounts from WT and *Ins2*^{Akita} mice, 24 hours after LPS injection and after in vivo P.I. staining. (A) A cluster of P.I.$^{+}$ vasculature (arrow) in LPS-treated *Ins2*^{Akita} mouse. (B) Quantitative analysis of P.I.$^{+}$ cells in retinal wholemounts. Data are expressed as mean ± SEM. N=7-10 mice per group. (C-D) High-power views featuring PI^{+} endothelium (arrows). Abbreviations: WT – wild type C57BL6/J-*Ins2*$^{+}$, AK – *Ins2*^{Akita}, LPS – lipopolysaccharide, PBS – phosphate-buffered saline, P.I. – propidium iodide.

Figure 3. **Ex vivo analysis of retinal leukostasis WT and *Ins2*^{Akita} mice, 24 hours post LPS injection.** (A) Rho-Con A staining of retinal vasculature in wholemount from WT PBS with x4 objective, (B) WT PBS under x20 objective and (C) AK PBS under x20 objective. (D) Rho-Con A staining highlights adherent leukocytes in retinal vasculature of WT LPS and (E) in wholemounts from AK LPS. (F) Quantitative analysis of adherent leukocytes in Rho-Con A stained retinal microvasculature in wholemounts. Data expressed as mean ± SEM. N=7-12 mice per group. Abbreviations: WT – wild type C57BL6/J-*Ins2*$^{+}$, AK – *Ins2*^{Akita}, LPS – lipopolysaccharide, PBS – phosphate-buffered saline.

Figure 4. In vivo analysis of total retinal thickness by optical coherence topography in 18 weeks old WT and *Ins2*^{Akita} mice after three doses of LPS. (A) Representative angiogram showing the nasal posterior retina of the right eye, with the optic cup as the reference. The horizontal green line is the en face view of the B-scan position. Vertical green lines represent distances from the optic disc at which measurements were made, i.e. from left to right 300µm, 600µm and 900µm from the center of the optic cup. (B) Representative

B-scan shows the normal laminar structure of the retina as a cross-sectional image. (C) The labeling of inner limiting membrane (ILM) and the location of Bruch's membrane (BM) with red segmentation lines is automated through the Heidelberg Eye Explorer software. All retinal thickness measurements from B-scans were plotted (vertical green lines) in the Heidelberg Eye Explorer according to the distance from the center of the optic cup. (D) Total retinal thickness in AK LPS in comparison to WT LPS mice at a distance of (E) 300µm, (F) 600µm or (F) 900µm from the optic cup. §= distance from the optic cup. N=8-13 mice per group. Data are presented as mean ± SEM. Abbreviations: WT – wild type C57BL6/J-*Ins2*$^{+}$, AK – *Ins2*^{Akita}, LPS – lipopolysaccharide, PBS – phosphate-buffered saline.

Figure 5. Image analysis of fluorescein angiograms in WT and *Ins2*^{Akita} mice after three doses of LPS. (A) Representative fluorescein angiograms of the deep and (B) intermediate vascular plexus, demonstrating uniform dense networks of well-defined capillaries. The white squares in plates A and B represent the sample areas in which the capillary outlines were manually traced (C), binarised (D) and skeletonised (E) prior to fractal analysis. Bar graphs demonstrate the average fractal dimensions in the deep (F) and intermedate (G) vascular networks. Data are presented as mean ± SEM. Scale bar = 200µm. N = 6 mice per group. Abbreviations: WT – wild type C57BL6/J-*Ins2*$^{+}$, AK – *Ins2*^{Akita}, LPS – lipopolysaccharide, PBS – phosphate-buffered saline.

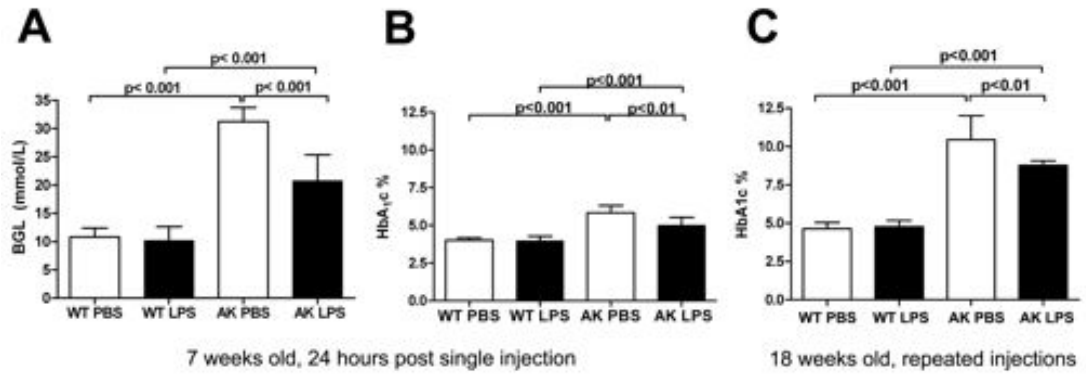
A
B
C
p< 0.001
p< 0.001
p< 0.001
BGL (mmol/L)
35
30
25
20
15
10
5
0
WT PBS
WT LPS
AK PBS
AK LPS
p<0.001
p<0.001
p<0.01
HbA1c %
12.5
10.0
7.5
5.0
2.5
0.0
7 weeks old, 24 hours post single injection
18 weeks old, repeated injections

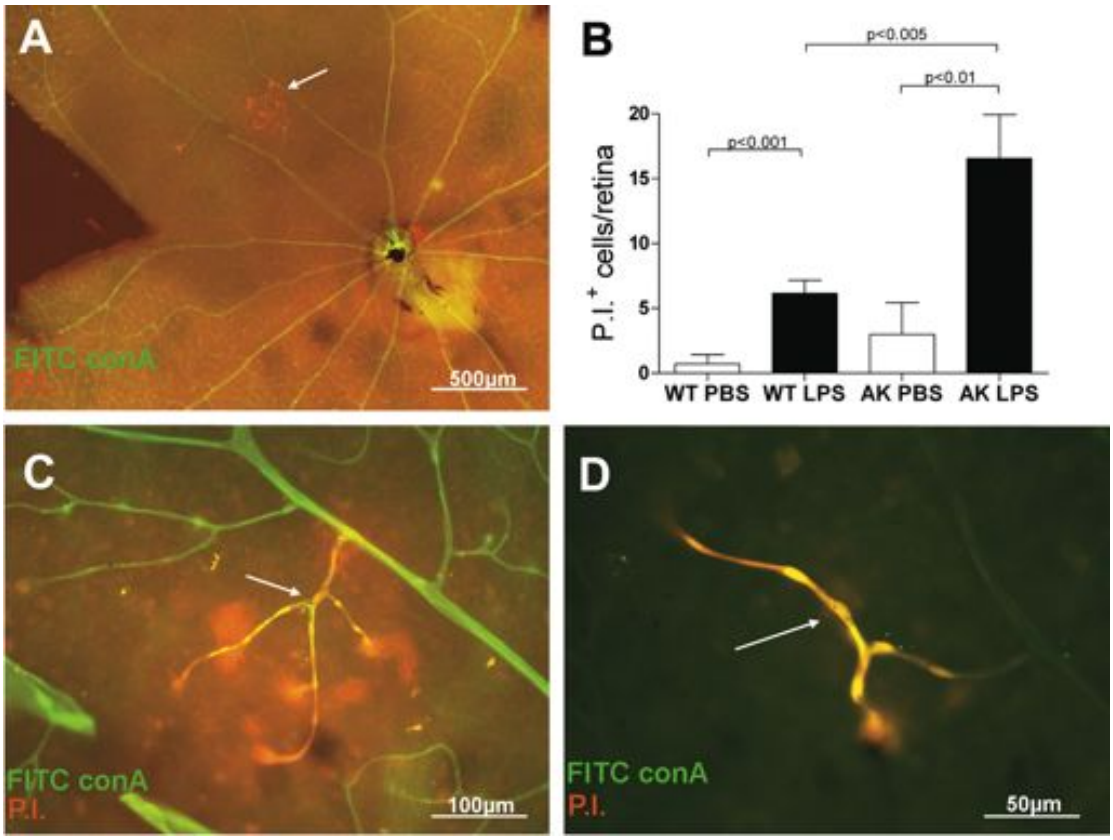
A
FITC conA
P.I.
500µm
B
p<0.005
p<0.01
p<0.001
P.I.+ cells/retina
20
15
10
5
0
WT PBS
WT LPS
AK PBS
AK LPS
C
FITC conA
P.I.
100µm
D
FITC conA
P.I.
50µm

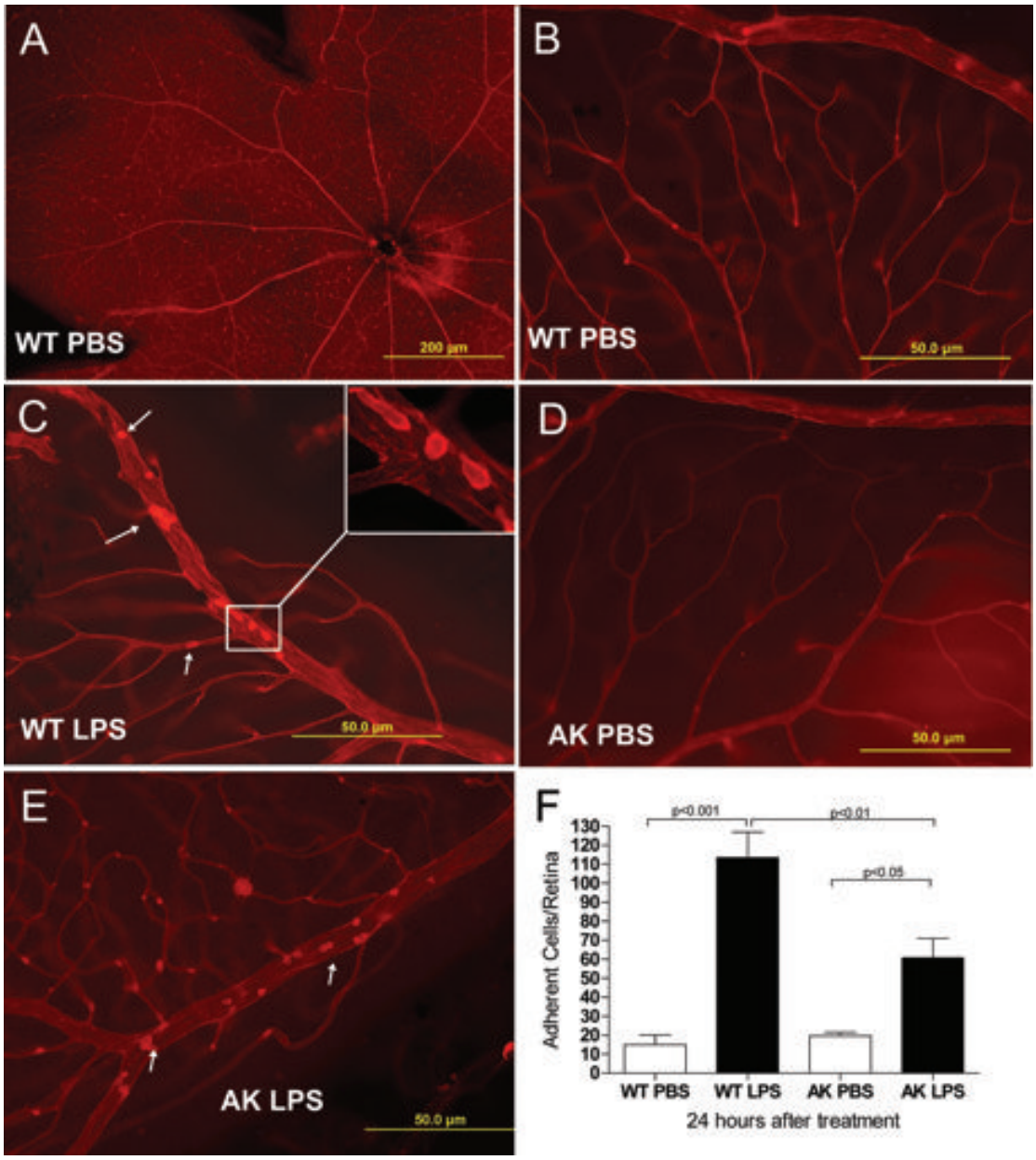
A
WT PBS
200 µm
B
WT PBS
50.0 µm
C
WT LPS
50.0 µm
D
AK PBS
50.0 µm
E
AK LPS
50.0 µm
F
p<0.001
p<0.01
p<0.05
Adherent Cells/Retina
130
120
110
100
90
80
70
60
50
40
30
20
10
0
WT PBS
WT LPS
AK PBS
AK LPS
24 hours after treatment

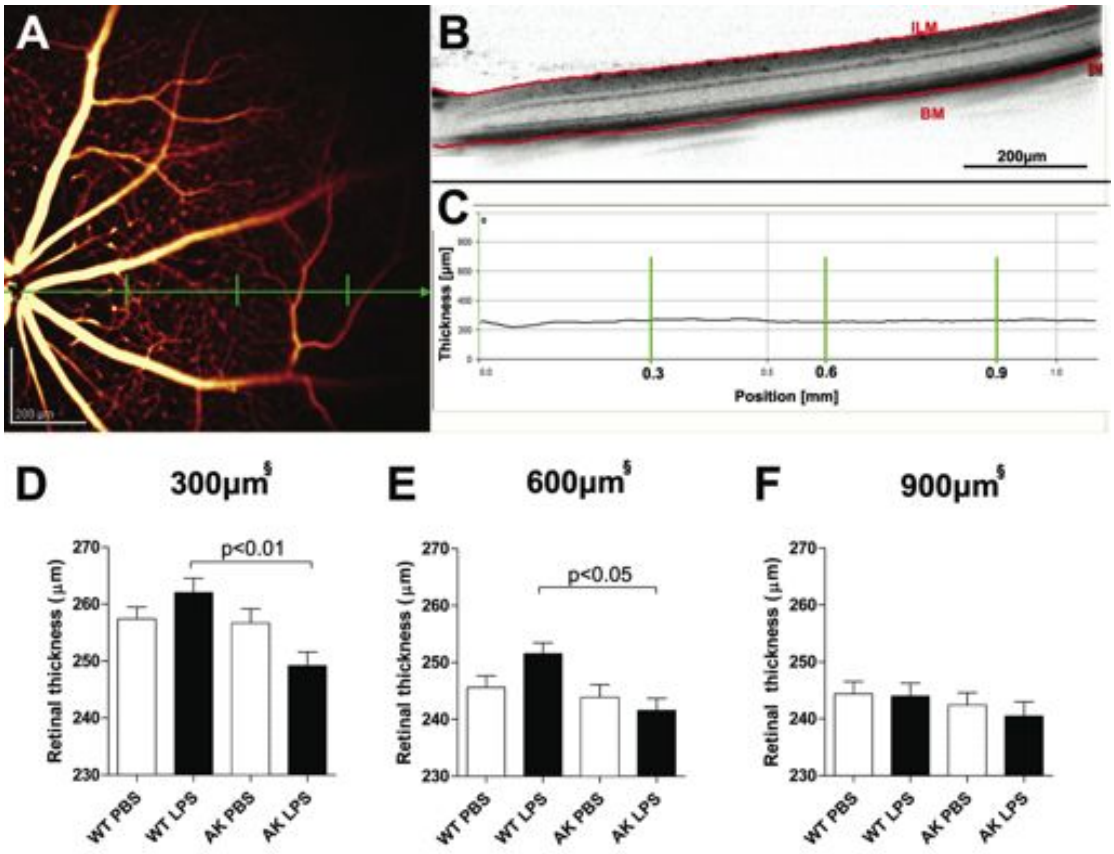
A
B
ILM
BM
200µm
C
Thickness [µm]
0.3
0.6
0.9
Position [mm]
D
300µm§
p<0.01
Retinal thickness (µm)
270
260
250
240
230
WT PBS
WT LPS
AK PBS
AK LPS
E
600µm§
p<0.05
Retinal thickness (µm)
270
260
250
240
230
WT PBS
WT LPS
AK PBS
AK LPS
F
900µm§
Retinal thickness (µm)
270
260
250
240
230
WT PBS
WT LPS
AK PBS
AK LPS

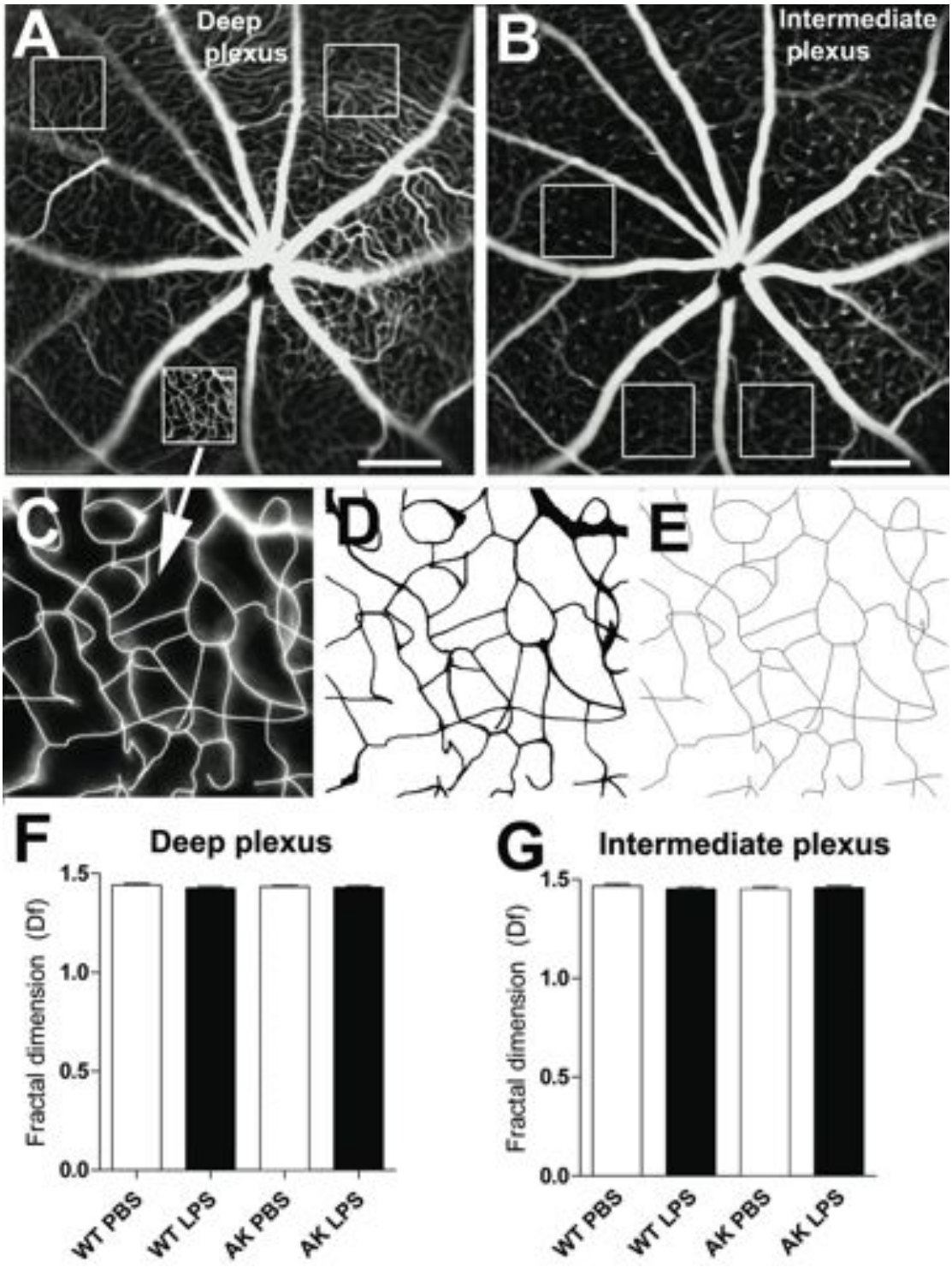
A
Deep plexus
B
Intermediate plexus
C
D
E
F
Deep plexus
Fractal dimension (Df)
1.5
1.0
0.5
0.0
WT PBS
WT LPS
AK PBS
AK LPS
G
Intermediate plexus
Fractal dimension (Df)
1.5
1.0
0.5
0.0
WT PBS
WT LPS
AK PBS
AK LPS